Integrated Satellite Multiple Two-way Relay Networks: Secrecy Performance under Multiple Eves and Vehicles with Non-ideal Hardware

Kefeng Guo, Xingwang Li, *Senior Member*, *IEEE*, Mamoun Alazab, *Senior Member*, *IEEE*, Rutvij H. Jhaveri, *Senior Member*, *IEEE*, and Kang An

***Abstract*—In this paper, we study the secrecy performance for an integrated satellite multiple two-way terrestrial relay network, where the non-ideal hardware, multiple vehicle eavesdroppers and multiple legitimate vehicle users are applied in the considered networks. To derive better secrecy performance, opportunistic terrestrial selection scheme is considered for the networks. Besides, the colluding eavesdropping scheme is also considered, where all the vehicle eaves work together to overhear the information. On these foundations, the closed-form expression for the secrecy outage probability is gotten. To obtain the further insights of system parameters and channel parameters in high signal-to-noise ratio regime, the asymptotic investigations for the secrecy outage probability is also investigated. At last, Monte Carlo results are given to show the efficiency and correctness of the analytical results.**

***Index Terms*—Integrated satellite multiple two-way terrestrial relay networks (ISMTTRNs), non-ideal hardware, multiple colluding eavesdroppers, multiple vehicle users, secrecy performance.**

I. Introduction

SATELLITE communication (SatCom) has been valued as the hopeful technology for the next generation (NG) wireless communication systems owing to its inherent characters, for example the wide coverage and high data rate to make the shortage of the ground relay systems. For some practical reasons, i.e. rain, fogs, and the other obstacles, the direct link is often not considered between the satellite and the terrestrial users/ vehicle users, relied on this foundation, the terrestrial/vehicle networks can make up this shortage of the SatCom [1]–[3]. Both utilizing the advantage of the terrestrial/vehicle networks and SatCom, the framework for the integrated satellite terrestrial relay networks (ISTRNs) appears [4], which has been applied in real networks, for example the Digital Video Broadcasting (DVB) networks [5], besides, ISTRNs are also cited in "Space-Ground Integrated Information Network Engineering" of China [6].

A. Literatures Review

ISTRNs have been the famous issue in the recent decades [1], [4], [7]–[13]. In [9], the authors analyzed the symbol error rate (SER) among a representative ISTRN. [10] researched the outage probability (OP) for the ISTRNs which suffers the non-ideal hardware. In [11], the authors analyzed the OP for a representative ISTRN along with the interference. [12] investigated the OP for the non-orthogonal multiple access (NOMA) based ISTRNs and made a great contribution for the NOMA technology. Moreover, there are several directions for the ISTRNs, for example, the authors in [13] researched the impact of reconfigurable intelligent surface(RIS)-based ISTRNs. As we all know that, satellite has a wide coverage, hence there are always many legitimate terrestrial relays/users/vehicles in one satellite beam. On this foundation, the investigation for the multiple terrestrial relays/users also becomes the hot topic [14], [15]. However, to have a balance between the performance and complexity, opportunistic terrestrial selection scheme, partial terrestrial relay selection scheme and the other threshold-based terrestrial relay selection scheme [4], [16]–[18] are proposed to solve this problem. Opportunistic terrestrial relay selection scheme can get the best system performance, however it needs the full channel state information (CSI) for all the transmission link [16]–[18]. However, partial terrestrial relay selection scheme gives the lower system complexity and acceptable system performance for it just needs the CSI either the source to the terrestrial relay or the terrestrial relay to the legitimate users, i.e., both the terrestrial users and vehicle users [19], [20]. While for the threshold-based terrestrial relay selection scheme, we can adjust the system complexity and system performance, which is the further researching direction for the terrestrial relay selection area. In [14], the OP was researched for a representative ISTRN which has multiple secondary users. The authors in [15] utilized the max-max user relay selection to a

This work was supported by the National Science Foundation of China under Grants 62001517 and 61901502, in part by the National Postdoctoral Program for Innovative Talents under Grant BX20200101, in part by the Key Scientific Research Projects of Higher Education Institutions in Henan Province under Grant 23B510001, in part by the Guangdong Basic and Applied Basic Research Foundation with grant number 2022A1515010999, in part by the Science and Technology Program of Guangzhou with grant number 202201011850, and in part by the Scientific Research Project of Education Department of Guangdong with grant number 2021KCXTD061.

K. Guo is with the School of Space Information, Space Engineering University, Beijing 101407, China (e-mail: guokefeng.cool@163.com).

X. Li is the School of Physics and Electronic Information Engineering, Henan Polytechnic University, Jiaozuo, 454000, China (e-mail: lixingwang-bupt@gmail.com).

M. Alazab, is with the College of Engineering, IT and Environment at Charles Darwin University, Melbourne, NT 0810, Australia (e-mail: alazab.m@ieee.org).

R. H. Jhaveri is with the Department of Computer Science and Engineering, School of Technology, Pandit Deendayal Energy University, Gandhinagar 382007, India (e-mail: rutvij.jhaveri@sot.pdpu.ac.in).

K. An is with the Sixty-third Research Institute, National University of Defense Technology, Nanjing, 210007, China (e-mail: ankang89@nudt.edu.cn).

representative ISTRN having multiple terrestrial relays/ users. In [19], the authors provided a terrestrial relay scheme for an uplink multiple terrestrial relay ISTRN. In [21], a threshold-based selection scheme was provided for the ISTRNs, when using this selection scheme, the OP was further analyzed. In [22], the ergodic capacity was researched for a representative ISTRN along with the partial selection scheme.

To enhance the spectrum efficiency and the time slot utilization, two-way technique is used for improving the spectrum utilization. The function of the two-way terrestrial relay is to transmit the signals to the source/destination simultaneously when compared with the one-way terrestrial relays [23]–[25]. [23] studied the OP for a representative ISTRN which has a terrestrial relay which worked in two-way mode. In [24], the OP was researched for the ISTRNs in the presence of many terrestrial two-way relays along with a proposed terrestrial selection scheme. [25] investigated the impacts of NOMA scheme and opportunistic terrestrial relay selection on the OP performance in the presence of many relays for a representative ISTRN.

As announced before, the transmission beam always has a wide coverage for both the terrestrial and satellite transmission nodes, thus there are many terrestrial/vehicle eavesdroppers existing in one transmission beam, which leads to the security problems [6], [26]. It is not similar with the traditional encryption techniques, physical layer security (PLS) is regarded to be a wishing way for analyzing the secure problems among the communication systems through wireless channel [27]. In [26], the authors concluded security issues in the SatComs. [18] proposed maximal user selection algorithm and analyzed the secrecy outage probability (SOP). In [8], the authors researched the SOP and secrecy energy efficiency in a representative NOMA-based ISTRNs, especially, the final expressions were further derived along with Monte Carlo (MC) simulations. In [28], the authors studied the secrecy issues for a representative ISTRN with the a proposed beamforming (BF) scheme and spectrum sharing. In [29], the authors researched the secrecy-energy efficient hybrid BF scheme for the millimeter wave-based ISTRNs. In [30], the authors investigated the security problem for the wireless powered cognitive ISTRNs with robust secure BF algorithm. [31] investigated the secrecy issue for the cognitive ISTRNs in the presence of underlay scheme and imperfect CSI. Till now, as the authors know that the secrecy problems on the two-way SatCom networks among the ISTRNs were first analyzed in [32], however it just considered the simple system model and ideal system considerations. Try the authors' best effort, there is few open works investigating the impact of two-way terrestrial relays on the secrecy ISTRNs with multiple terrestrial/vehicle eavesdroppers.

B. Motivation of This Paper

In practical systems, the networks nodes are not always perfect, which means they always suffer the phase noise, I/Q imbalance, and amplifier non-linearities [33]–[35], which results in the non-ideal hardware i.e., hardware impairments (HIs) of the practical systems. [36] concluded all the issues and gave a famous widely used HIs model [37]–[39]. In [40], the authors researched the influence of HIs on the SatComs and obtained the closed-form expression for the OP. The impact of HIs on the ISTRNs has been investigated in [4], [8], [19], [20], [40]. In these papers, the terrestrial relay selection scheme, two-way terrestrial relays, cognitive radio, NOMA, and the other technology are all investigated, which indicate that HIs is a hot topic that needs to be researched. Furthermore, the research of HIs on the secrecy problems is also the popular direction, which has been studied in [41]–[43]. Try the authors' best knowledge, the secrecy issues with HIs for the ISTRNs were major reported in [8], [44]. In [8], the influence of HIs on the NOMA-based ISTRNs was researched. Moreover, we should have a clear mind that the former works mainly focus on the impact of one-way terrestrial relay for the ISTRNs, the investigation for an ISTRN with multiple two-way terrestrial relays in the presence of HIs remains unreported, especially in the presence of many vehicle legitimate users and multiple vehicle eves.

C. Our Contributions

Motivated by these observations, by taking both HIs and two-way terrestrial relays into our sight, we study secrecy performance of ISTRNs with multiple terrestrial relays employing opportunistic terrestrial selection scheme, particularly, many legitimate vehicle users and multiple vehicle eavesdroppers are considered. The detailed contributions of this work are shown in what follows:

- By considering the HIs and two-way terrestrial relay into our sight, we give a framework of the secrecy integrated satellite multiple two-way terrestrial relay networks (ISMTTRNs), where several terrestrial relays, several legitimate vehicle users, and multiple vehicle eavesdroppers are considered. Besides, decode-and-forward (DF) protocol is applied at terrestrial relays to assist the source forward the transmission information. The satellite transmission link, the terrestrial transmission link and the vehicle eavesdropping link are considered to suffer shadowed-Rician (SR) and Rayleigh fading, respectively.
- Upon the considered network, we obtain the closed-form expression for the SOP with colluding eavesdropping scheme. To achieve the best secrecy performance, opportunistic relay selection algorithm was used for the considered system. In addition, the detailed analysis for SOP is further obtained, from which we can investigate the SOP easily, these theoretical results can also direct the engineering guide.
- Simple yet tight asymptotic analysis is derived to valuate the impact of HIs in high signal-to-noise ratio (SNR) regime, on this foundation, the secrecy diversity order and secrecy coding gain are further obtained. Furthermore, two characters are investigated from these analysis. Firstly, HIs does not have influence on the secrecy diversity, however they will seriously reduce the secrecy coding gain of the networks, thus affecting the secrecy system performance. Secondly, opportunistic terrestrial relay selection scheme has great impact on the secrecy performance.

This article has been accepted for publication in IEEE Transactions on Intelligent Vehicles. This is the author's version which has not been fully edited and content may change prior to final publication. Citation information: DOI 10.1109/TIV.2022.3215011

TABLE I
ACRONYMS AND ABBREVIATIONS

Acronym	Definition
AS	average shadowing
AWGN	additive white Gaussian noise
BF	beamforming
CDF	cumulative distribution function
CSI	channel state information
DF	decode-and-forward
DVB	Digital Video Broadcasting
FHS	frequent heavy shadowing
FSL	free space loss
GEO	geosynchronous Earth orbit
HIs	hardware impairments
ILS	infrequent light shadowing
ISMTTRNs	integrated satellite multiple two-way terrestrial relay networks
ISTRNs	integrated satellite terrestrial relay networks
LMS	land mobile satellite
LOS	line of sight
MC	Monte Carlo
NG	next generation
NOMA	non-orthogonal multiple access
OP	outage probability
PDF	probability density function
PLS	physical layer security
RIS	reconfigurable intelligent surface
SatCom	satellite communication
SER	symbol error rate
SINDR	signal-to-interference-and-noise plus distortion ratio
SNDR	signal-to-noise and distortion ratio
SNR	signal-to-noise ratio
SOP	secrecy outage probability
SR	shadowed-Rician
TDMA	time division multiple access

The following parts of this work provided as: the system model was illustrated in Section II. The secrecy system performance is analyzed in Section III. For Section IV, representative MC simulation results are derived to prove the theoretical results. During Section V, a conclusion of this paper is derived.

D. Notations

$\exp(\cdot)$ represents the exponential function, $E[\cdot]$ is the expectation operator. $f_x(\cdot)$ and $F_x(\cdot)$ are the probability density function (PDF) and the cumulative distribution function (CDF) of random variable x, respectively. The acronyms and abbreviations are provided in Table I.

II. SYSTEM MODEL AND PROBLEM FORMULATION

As presented in Fig. 1, in this paper, we introduce a secrecy ISTRN into our consideration, where a source satellite (S_1), multiple source vehicle users ($S_{2i}, i \in \{1, \ldots, N\}$), multiple two-way terrestrial relays ($R_p, p \in \{1, \ldots, M\}$), multiple vehicle eavesdroppers ($E_j, j \in \{1, \ldots, L\}$). Due to the heavy fading, rain, fogs, and the other reasons, there is no direct link between the S_1 and S_{2i} for S_{2i} is not in the coverage of the transmission beam of S_1. Besides, all the transmission nodes in this paper are assumed to own only one antenna[1]. All the terrestrial relays work in DF protocol. In addition, maximal selection scheme is applied into the S_{2i}, which means the best user is selected for the transmission. The eavesdroppers can both overhear the signals from S_1 and S_{2i}.

[1]It is considered that, for the considered network, each transmission node has a single antenna. However, the derived important results are further suitable for the case with several antennas after the suitable BF scheme is applied.

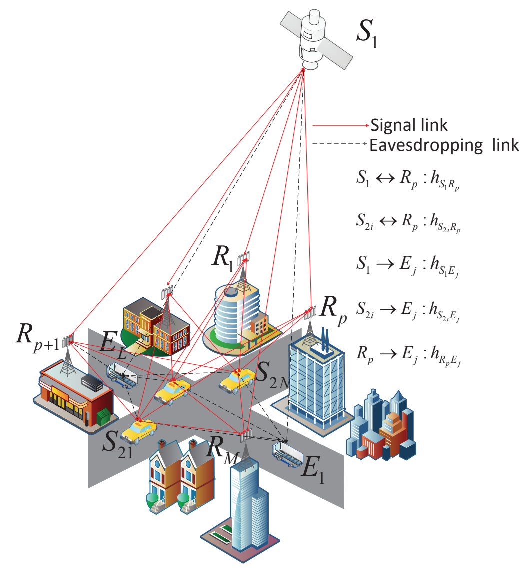

Fig. 1. Illustration of the system model

It requires two time slots through the total transmission. For the first time slot, the signal $s_1(t)$ with $E\left[|s_1(t)|^2\right] = 1$ from S_1 and the information signal $s_{2i}(t)$ with $E\left[|s_{2i}(t)|^2\right] = 1$ from S_{2i} is transmitted to p-th R simultaneously, respectively. Thus, the received signal at the p-th R is presented as[2]

$$\begin{aligned} y_{R_p}(t) &= \sqrt{P_{S_1}} h_{S_1R_p}\left[s_1(t) + \eta_1(t)\right] \\ &\quad + \sqrt{P_{S_{2i}}} h_{S_{2i}R_p}\left[s_{2i}(t) + \eta_{2i}(t)\right] + n_{R_p}(t), \end{aligned} \tag{1}$$

where P_{S_1} is the transmission power from S_1, $P_{S_{2i}}$ denotes the transmission power from i-th S_2 namely S_{2i}. $h_{S_1R_p}$ represents the channel fading between S_1 and the p-th R obeying the SR fading, $h_{S_{2i}R_p}$ is the channel fading between S_{2i} and the p-th R with distributing as Rayleigh fading. As presented before, the network nodes suffer the HIs, $\eta_1(t)$ and $\eta_{2i}(t)$ denote the distortion noise owing to HIs at S_1 and S_{2i}, respectively, which are shown as $\eta_1(t) \sim \mathcal{CN}\left(0, k_1^2\right)$ and $\eta_{2i}(t) \sim \mathcal{CN}\left(0, k_{2i}^2\right)$. k_1 and k_{2i} denote the HIs level at the S_1 and S_{2i}, respectively [4], [40]. $n_{R_p}(t)$ represents the additive white Gaussian noise (AWGN) at the p-th R which is represented as $n_{R_p}(t) \sim \mathcal{CN}\left(0, \delta_{R_p}^2\right)$.

As shown before, the secrecy problems exist in the wireless communication networks, thus the received signal at the vehicle eavesdroppers[3] are shown as

$$y_E(t) = \sum_{j=1}^{L} \sqrt{P_{S_1}} h_{S_1E_j}\left[s_1(t) + \eta_1(t)\right]$$

[2]In this paper, maximal user scheduling scheme is used in the considered system, thus after the channel estimation, the vehicle user with best performance is selected for the transmission. In (1), $s_{2i}(t)$ is the selected signal and the i-th S_2 is the selected vehicle.

[3]In the considered system model, colluding scheme is employed for the eavesdroppers, thus the eavesdropping signal is the sum of received signals by all vehicle eavesdroppers.

$$+\sum_{j=1}^{L}\sqrt{P_{S_{2i}}}h_{S_{2i}E_j}\left[s_{2i}\left(t\right)+\eta_{2i}\left(t\right)\right]+n_{E_j}\left(t\right), \quad (2)$$

where $h_{S_1E_j}$ represents the channel fading between S_1 and the j-th E that undergoes the SR fading, $h_{S_{2i}E_j}$ represents the channel fading between S_{2i} and the j-th E with distributing as Rayleigh fading. $n_{E_j}\left(t\right)$ denotes the AWGN at the j-th E which is shown as $n_{E_j}\left(t\right)\sim\mathcal{CN}\left(0,\delta^2_{E_j}\right)$.

For the second transmission slot, the p-th R re-transmits the obtained signal to the two sources respectively in the presence of DF protocol, which results in that the derived signal at S_{2i} is given by[4]

$$y_{S_{2i}}\left(t\right)=\sqrt{P_{R_p}}h_{S_{2i}R_p}\left[s_1\left(t\right)+\eta_{R_p}\left(t\right)\right]+n_{S_{2i}}\left(t\right), \quad (3)$$

where P_{R_p} represents the transmission power of the p-th R, $\eta_{R_p}\left(t\right)$ depicts the distortion noise due to HIs with distributing as $\eta_{R_p}(t)\sim\mathcal{CN}\left(0,k^2_{R_p}\right)$ with k_{R_p} being the distortion level for the p-th R [4], [40]. $n_{S_{2i}}\left(t\right)$ represents the AWGN at the i-th S_2 which has the form as $n_{S_{2i}}\left(t\right)\sim\mathcal{CN}\left(0,\delta^2_{S_{2i}}\right)$.

With the similar method, the obtained signal at S_1 is given by

$$y_{S_1}\left(t\right)=\sqrt{P_{R_p}}h_{S_1R_p}\left[s_{2i}\left(t\right)+\eta_{R_p}\left(t\right)\right]+n_{S_1}\left(t\right), \quad (4)$$

where $n_{S_1}\left(t\right)$ represents the AWGN at the S_1 which is shown as $n_{S_1}\left(t\right)\sim\mathcal{CN}\left(0,\delta^2_{S_1}\right)$.

The received signal at the vehicle eavesdroppers through the second time slot for downlink is given by

$$y_{R_pE}\left(t\right)=\sum_{j=1}^{L}\sqrt{P_{R_p}}h_{R_pE_j}\left[s_1\left(t\right)+\eta_{R_p}\left(t\right)\right]+n_{E_j}\left(t\right), \quad (5)$$

where $h_{R_pE_j}$ denotes the channel fading between the p-th R and the j-th E that obeys the Rayleigh fading.

For uplink, the derived signal for the vehicle eavesdroppers is presented as

$$y_{R_pE}\left(t\right)=\sum_{j=1}^{L}\sqrt{P_{R_p}}h_{R_pE_j}\left[s_{2i}\left(t\right)+\eta_{R_p}\left(t\right)\right]+n_{E_j}\left(t\right). \quad (6)$$

By utilizing (1), the obtained signal-to-interference-and-noise plus distortion ratio (SINDR) for decrypting $s_1\left(t\right)$ and $s_{2i}\left(t\right)$ are, respectively, given by

$$\gamma_{S_1\to R_p}=\frac{P_{S_1}\left|h_{S_1R_p}\right|^2}{P_{S_1}\left|h_{S_1R_p}\right|^2k_1^2+P_{S_{2i}}\left|h_{S_2R_p}\right|^2(1+k^2_{2i})+\delta^2_{R_p}}=\frac{\lambda_{S_1R_p}}{\lambda_{S_1R_p}k_1^2+\lambda_{S_2R_p}\left(1+k^2_{2i}\right)+1}, \quad (7)$$

$$\gamma_{S_2\to R_p}=\frac{\lambda_{S_2R_p}}{\lambda_{S_1R_p}\left(1+k_1^2\right)+\lambda_{S_2R_p}k^2_{2i}+1}, \quad (8)$$

where $\lambda_{S_1R_p}=\frac{P_{S_1}\left|h_{S_1R_p}\right|^2}{\delta^2_{R_p}}$ and $\lambda_{S_2R_p}=\max\limits_{i\in\{1,\dots,N\}}\left(\lambda_{S_{2i}R_p}\right)=\max\limits_{i\in\{1,\dots,N\}}\frac{P_{S_{2i}}\left|h_{S_{2i}R_p}\right|^2}{\delta^2_{R_p}}$.

From (2), the signal-to-noise and distortion ratio (SNDR) at the E for the downlink and uplink are, respectively, given as

$$\gamma_{S_1\to E}=\frac{\lambda_{S_1E}}{\lambda_{S_1E}k_1^2+1}, \quad (9)$$

$$\gamma_{S_{2i}\to E}=\frac{\lambda_{S_{2i}E}}{\lambda_{S_{2i}E}k^2_{2i}+1}, \quad (10)$$

where $\lambda_{S_1E}=\frac{P_{S_1}\sum_{j=1}^{L}\left|h_{S_1E_j}\right|^2}{\delta^2_{E_j}}$ and $\lambda_{S_{2i}E}=\frac{P_{S_{2i}}\sum_{j=1}^{L}\left|h_{S_{2i}E_j}\right|^2}{\delta^2_{E_j}}$.

In the second time slot, from (3) and (4), the obtained SNDR are, respectively, derived as

$$\gamma_{R_p\to S_2}=\frac{\lambda_{R_pS_2}}{\lambda_{R_pS_2}k^2_{R_p}+1}, \quad (11)$$

$$\gamma_{R_p\to S_1}=\frac{\lambda_{R_pS_1}}{\lambda_{R_pS_1}k^2_{R_p}+1}, \quad (12)$$

where $\lambda_{R_pS_2}=\max\limits_{i\in\{1,\dots,N\}}\left(\frac{P_{R_p}\left|h_{S_{2i}R_p}\right|^2}{\delta^2_{2i}}\right)=\max\limits_{i\in\{1,\dots,N\}}\left(\lambda_{R_pS_{2i}}\right)$ and $\lambda_{R_pS_1}=\frac{P_{R_p}\left|h_{S_1R_p}\right|^2}{\delta^2_1}$.

With the help of (6), the SNDR at vehicle eavesdroppers for the second time slot is obtained as

$$\gamma_{R_p\to E}=\frac{\lambda_{R_pE}}{\lambda_{R_pE}k^2_{R_p}+1}, \quad (13)$$

where $\lambda_{R_pE}=\sum_{j=1}^{L}\frac{P_{R_p}\left|h_{R_pE_j}\right|^2\left|s_1(t)\right|^2}{\delta^2_{E_j}}=\sum_{j=1}^{L}\frac{P_{R_p}\left|h_{R_pE_j}\right|^2\left|s_{2i}(t)\right|^2}{\delta^2_{E_j}}=\sum_{j=1}^{L}\lambda_{R_pE_j}$.

According to [42], by utilizing the opportunistic terrestrial relay selection scheme and (7), (8), (9), (10), (11), (12), (13), the secrecy capacity for the whole network is written as

$$C_S=\max_{p\in\{1,\dots,M\}}\left\{\min\left[C_{S_1},C_{S_2}\right]^+\right\}, \quad (14)$$

where $[x]^+=\max(x,0)$, $C_{S_1}=\min\left(C_{S_{11}},C_{S_{12}}\right)$, $C_{S_2}=\min\left(C_{S_{21}},C_{S_{22}}\right)$, $C_{S_{11}}=\log_2\left(1+\gamma_{S_1\to R_p}\right)-\log_2\left(1+\gamma_{S_1\to E}\right)$, $C_{S_{22}}=\log_2\left(1+\gamma_{R_p\to S_2}\right)-\log_2\left(1+\gamma_{R_p\to E}\right)$, $C_{S_{12}}=\log_2\left(1+\gamma_{S_2\to R_p}\right)-\log_2\left(1+\gamma_{S_{2i}\to E}\right)$ and $C_{S_{21}}=\log_2\left(1+\gamma_{R_p\to S_1}\right)-\log_2\left(1+\gamma_{R_p\to E}\right)$.

III. Secrecy Performance Analysis

The detailed analysis for the SOP will be given in this section. At first, the channel model for the transmission link are presented.

A. The Channel Model

1) Terrestrial Transmission Link Model: Shown from the network, the channel model for the terrestrial/vehicle transmission link is considered as independent and identically distribution (i.i.d) Rayleigh fading. Recalling [1], so the PDF and CDF of $\lambda_V, V\in\{S_{2i}R_p, R_pE_j, R_pS_{2i}\}$, are, respectively, given by

$$f_{\lambda_V}\left(x\right)=\frac{1}{\bar{\lambda}_V}e^{-\frac{x}{\bar{\lambda}_V}} \quad (15)$$

[4] As S_{2i} knows its own signal, thus in Eq. (3), the signal $s_{2i}\left(t\right)$ is eliminated [1], [8].

and

$$F_{\lambda_V}(x) = 1 - e^{-\frac{x}{\bar{\lambda}_V}}, \tag{16}$$

where $\bar{\lambda}_V$ represents the average channel gain.

Based on [8], the PDF for $\lambda_Q, Q \in \{S_{2i}E, R_pE\}$ is derived as

$$f_{\lambda_Q}(x) = \sum_{i=1}^{\rho(A_Q)} \sum_{j=1}^{\tau_i(A_Q)} \frac{\chi_{i,j}(A_Q)\,\mu_{\langle i\rangle}^{-j}}{(j-1)!} x^{j-1} e^{-x/\mu\langle i\rangle}, \tag{17}$$

where $A_Q = diag(\mu_1, \ldots, \mu_i, \ldots, \mu_L)$, $\rho(A_Q)$ depicts the number of distinct diagonal elements of A_Q, $\mu_{\langle 1\rangle} > \mu_{\langle 2\rangle} > \cdots > \mu_{\langle \rho(A_Q)\rangle}$ represents the ascending order of $\mu\langle i\rangle$, $\tau_i(A_Q)$ denotes the multiplicity of $\mu\langle i\rangle$, and $\chi_{i,j}(A_Q)$ represents the (i,j)-th characteristic coefficient of A_Q [8].

Besides, with the help of [32] and maximal vehicle user selection scheme, the CDF and PDF for $\lambda_X, X \in \{S_2R_p, R_pS_2\}$ are derived as

$$F_{\lambda_X}(x) = \left(1 - e^{-\frac{x}{\bar{\lambda}_V}}\right)^N = \sum_{q=0}^{N} \binom{N}{q} (-1)^q e^{-\frac{qx}{\bar{\lambda}_X}}, \tag{18}$$

$$f_{\lambda_X}(x) = \frac{N}{\bar{\lambda}_X} \sum_{q=0}^{N-1} \binom{N-1}{q} (-1)^q e^{-\frac{(q+1)x}{\bar{\lambda}_X}}. \tag{19}$$

2) The Satellite Channel Model: Through the whole work, the geosynchronous Earth orbit (GEO) satellite is selected for the analysis. Besides, we also assume that the satellite owns multiple beams for the considered system model. Besides, time division multiple access (TDMA)[5] [45] is utilized for the analyzed network, which means that only one terrestrial R is used to transmit the signal for each time slot.

$h_O, O \in \{\{S_1R_p\}, \{S_1E_j\}\}$ depicts the channel coefficient between the down-link on-board satellite beam and terrestrial relay/vegicle eavesdroppers, which is derived as

$$h_O = C_O f_O, \tag{20}$$

where f_O is applied as the random SR factor, and C_O represents the effects of the antenna pattern and free space loss (FSL) with the presentation as

$$C_O = \frac{c\sqrt{G_O G_R}}{8\pi^2 f \sqrt{d^2 + d_0^2}}, \tag{21}$$

where c represents the transmission speed for the frequency carrier, f denotes the transmission frequency. d depicts the length between the terrestrial relays/vehicle eavesdroppers and the satellite's center. $d_0 \approx 35786km$, G_O denotes the antenna gain for the relays/vehicle eavesdroppers, what's more, G_R is considered as the satellite's on-board beam gain.

By considering [40], G_R is re-presented as

$$G_R(dB) \simeq \begin{cases} \overline{G}_{\max}, & for\ 0^\circ < \vartheta < 1^\circ \\ 32 - 25\log\vartheta, & for\ 1^\circ < \vartheta < 48^\circ \\ -10, & for\ 48^\circ < \vartheta \le 180^\circ, \end{cases} \tag{22}$$

where $\overline{G}_{\max}$ in considered to be the maximum beam gain with ϑ being the angle for the off-boresight. When considering G_O, with assuming θ_k being the transmission angle. $\bar{\theta}_k$ denotes the on-board beam 3dB angle. Besides, the antenna gain G_O is presented as [4], [40]

$$G_O \simeq G_{\max}\left(\frac{K_1(u_k)}{2u_k} + 36\frac{K_3(u_k)}{u_k^3}\right), \tag{23}$$

where G_{max} represents the maximal beam gain, $u_k = 2.07123\sin\theta_k/\sin\overline{\theta}_k$, K_1 and K_3 denote the 1st-kind bessel function of order 1 and 3, respectively. To achieve the largest beam gain, $\theta_k \to 0$ is considered leading to $G_O \approx G_{\max}$. Relied on this foundation, we obtain $h_O = C_O^{\max} f_O$.

For f_O, one famous SR model was given in [1], which is utilized for land mobile satellite (LMS) communication [42]. By using [40], f_O can be re-given as $f_O = \overline{f}_O + \widetilde{f}_O$, where $\widetilde{f}_O$ is considered to suffers the i.i.d Rayleigh fading distribution while $\overline{f}_O$ depicts the element of line-of-sight (LOS) component which undergoes i.i.d Nakagami-m shadowing.

Besides, the PDF of $\lambda_O = \overline{\lambda}_O |C_O^{\max} f_O|$ is derived as

$$f_{\lambda_O}(x) = \sum_{k_1=0}^{m_O-1} \frac{\alpha_O (1-m_O)_{k_1} (-\delta_O)^{k_1} x^{k_1}}{(k_1!)^2 \overline{\lambda}_O^{k_1+1} \exp(\Delta_O x)}, \tag{24}$$

where $\overline{\lambda}_O$ denotes the average signal-to-noise ratio (SNR) from the satellite to legitimate vehicle users/vehicle eavesdroppers, $\Delta_O = \frac{\beta_O - \sigma_O}{\overline{\lambda}_O}$, $\alpha_O = \left(\frac{2b_O m_O}{2b_O m_O + \Omega_O}\right)^{m_O} / 2b_O$, $\beta_O = 1/2b_O$, $\delta_O = \frac{\Omega_O}{(2b_O m_O + \Omega_O) 2b_O}$, where $m_O \ge 0$ represents the fading severity parameter, $2b_O$ is the average power of the multipath component and Ω_O depicts the average power for the LOS component. As a widely assumption, in this paper, m_O is considered to be an integer [14]. $(\cdot)_{k_1}$ denotes the Pochhammer symbol [46].

Relied on (24) and using [15], the CDF of λ_O can be written as

$$F_{\lambda_O}(x) = 1 - \sum_{k_1=0}^{m_O-1} \sum_{t=0}^{k_1} \frac{\alpha_O (1-m_O)_{k_1} (-\delta_O)^{k_1} x^t}{k_1! t! \overline{\lambda}_O^{k_1+1} \Delta_O^{k_1-t+1} \exp(\Delta_O x)}. \tag{25}$$

From [23]. the PDF of λ_{S_1E} can be obtained as

$$f_{\lambda_{S_1E}}(x) = \sum_{\xi_1=0}^{m_{S_1E}-1} \cdots \sum_{\xi_L=0}^{m_{S_1E}-1} \Xi(L)\, x^{\Lambda_{S_1E}-1} \exp(-\Delta_{S_1E} x), \tag{26}$$

where

$$\Xi(L) \triangleq \prod_{\tau=1}^{L} \varsigma(\xi_\tau) a_{S_1E}^L \prod_{\ell=1}^{L-1} B\left(\sum_{l=1}^{\ell} \xi_l + \ell, \xi_{l+1} + 1\right),$$

$\Lambda_{S_1E} \triangleq \sum_{\tau=1}^{L} \xi_\tau + L$, $\varsigma(\xi_\tau) = \frac{(1-m_{S_1E})_{\xi_\tau} (-\delta_{S_1E})^{\xi_\tau}}{(\xi_\tau!)^2 \overline{\lambda}_{S_1E}^{\xi_\tau+1}}$, $\Delta_{S_1E} = \frac{\beta_{S_1E} - \alpha_{S_1E}}{\overline{\lambda}_{S_1E}}$, $\alpha_{S_1E} = \left(\frac{2b_{S_1E} m_{S_1E}}{2b_{S_1E} m_{S_1E} + \Omega_{S_1E}}\right)^{m_{S_1E}} / 2b_{S_1E}$, $\beta_{S_1E} = 1/2b_{S_1E}$, $\delta_{S_1E} = \frac{\Omega_{S_1E}}{(2b_{S_1E} m_{S_1E} + \Omega_{S_1E}) 2b_{S_1E}}$ and $B(.,.)$ denotes the Beta function [46].

[5]TDMA scheme is used in the satellite to keep only one satellite beam and one terrestrial two-way relay node is used in each data transmission time slot. TDMA scheme is both adopted for the satellite downlink and uplink data transmission.

This article has been accepted for publication in IEEE Transactions on Intelligent Vehicles. This is the author's version which has not been fully edited and content may change prior to final publication. Citation information: DOI 10.1109/TIV.2022.3215011

B. Secrecy Outage Probability

From [1], the SOP can be defined as

$$\begin{aligned}\Pr\left(C_S \le C_0\right) &= \left\{\Pr\left\{\left\{\min\left[C_{S_1}, C_{S_2}\right]^+\right\} \le C_0\right\}\right\}^M \\ &= \left[\Pr\left(C_{S_1} \le C_0\right) + \Pr\left(C_{S_1} \le C_0\right)\right. \\ &\quad \left.- \Pr\left(C_{S_1} \le C_0\right)\Pr\left(C_{S_2} \le C_0\right)\right]^M, \end{aligned} \tag{27}$$

where $C_0 = \log_2\left(1+\gamma_0\right)$ with γ_0 being the target threshold.

Then, the closed-form expressions for the SOP is obtained in **Theorem 1**.

Theorem 1.

$$\begin{aligned}\Pr\left(C_S \le C_0\right) &= \Pr\left(C_{S_{11}} \le C_0\right) + \Pr\left(C_{S_{22}} \le C_0\right) \\ &\quad - \Pr\left(C_{S_{11}} \le C_0\right)\Pr\left(C_{S_{22}} \le C_0\right) \\ &\quad + \Pr\left(C_{S_{12}} \le C_0\right) + \Pr\left(C_{S_{21}} \le C_0\right) \\ &\quad - \Pr\left(C_{S_{12}} \le C_0\right)\Pr\left(C_{S_{21}} \le C_0\right) \\ &\quad - \left[\Pr\left(C_{S_{11}} \le C_0\right) + \Pr\left(C_{S_{22}} \le C_0\right)\right. \\ &\quad \left.- \Pr\left(C_{S_{11}} \le C_0\right)\Pr\left(C_{S_{22}} \le C_0\right)\right] \\ &\quad \times \left[\Pr\left(C_{S_{12}} \le C_0\right) + \Pr\left(C_{S_{21}} \le C_0\right)\right. \\ &\quad \left.- \Pr\left(C_{S_{12}} \le C_0\right)\Pr\left(C_{S_{21}} \le C_0\right)\right], \end{aligned} \tag{28}$$

where $\Pr\left(C_{S_{11}} \le C_0\right)$ *is shown as* (29)*, which is shown at the top of next page. In* (29)*,* $H_1\left(z\right)$ *is written as*

$$\begin{aligned}H_1\left(z\right) &= \exp\left(-\frac{\Delta_{m_{S_1R_p,k}} z}{1-k_1^2 z} - \frac{\Delta_{S_1E} z}{1-k_1^2 z}\right)\frac{z^{t+\Lambda_{S_1E}-1}}{\left(1-k_1^2 z\right)^{t+3-\Lambda_{S_1E}}} \\ &\quad \times \left[\frac{\Delta_{m_{S_1R_p,k}}\left(1+k_{2i}^2\right) z}{1-k_1^2 z} + \frac{q+1}{\bar{\lambda}_{S_2R_p}}\right]^{-p-1}. \end{aligned} \tag{30}$$

$\Pr\left(C_{S_{22}} \le C_0\right)$ *is shown as* (31)*, which is shown at the top of next page. In* (31)*,* $H_2\left(z\right)$ *is derived as*

$$\begin{aligned}H_2\left(z\right) &= e^{-\frac{q\left[z\left(1+\gamma_0\right)+\gamma_0\right]}{\bar{\lambda}_{R_pS_2}\left\{1-\left[k_{R_p}^2 z\left(1+\gamma_0\right)+\gamma_0\right]\right\}}}\left(\frac{z}{1-k_{R_p}^2 z}\right)^{j-1} \\ &\quad \times e^{-z/\left[\left(1-k_{R_p}^2 z\right)\mu\langle i\rangle\right]}. \end{aligned} \tag{32}$$

$\Pr\left(C_{S_{12}} \le C_0\right)$ *is shown as* (33)*, which is presented at the top of next page. In* (33)*,* $H_3\left(z\right)$ *is represented as*

$$\begin{aligned}H_3\left(y\right) &= \exp\left(-\frac{q\left[y\left(1+\gamma_0\right)+\gamma_0\right]}{\left(1-k_{2i}^2\left[y\left(1+\gamma_0\right)+\gamma_0\right]\right)\bar{\lambda}_{S_2R_p}}\right) \\ &\quad \times \exp\left(-\frac{y}{\left(1-k_{2i}^2 y\right)\mu\left\langle i\right\rangle}\right)\frac{y^{j-1}}{\left(1-k_{2i}^2 y\right)^{j+1}} \\ &\quad \times \left(\Delta_{S_1R_p} + \frac{q\left[y\left(1+\gamma_0\right)+\gamma_0\right]\left(1+k_1^2\right)}{\left(1-k_{2i}^2\left[y\left(1+\gamma_0\right)+\gamma_0\right]\right)\bar{\lambda}_{S_2R_p}}\right)^{-k_1-1} \end{aligned} \tag{34}$$

$\Pr\left(C_{S_{21}} \le C_0\right)$ *is shown as* (35)*, which is presented in the middle of next page. In* (35)*,* $H_4\left(z\right)$ *is represented as*

$$\begin{aligned}H_4\left(z\right) &= \left\{\frac{y\left(1+\gamma_0\right)+\gamma_0}{1-k_{R_p}^2\left[y\left(1+\gamma_0\right)+\gamma_0\right]}\right\}^t \frac{y^{j-1}e^{-\frac{y}{\left(1-k_{R_p}^2 y\right)\mu\langle i\rangle}}}{\left(1-k_{R_p}^2 y\right)^{j+1}} \\ &\quad \times \exp\left\{-\frac{\Delta_{R_pS_1,k}\left[y\left(1+\gamma_0\right)+\gamma_0\right]}{1-k_{R_p}^2\left[y\left(1+\gamma_0\right)+\gamma_0\right]}\right\}. \end{aligned} \tag{36}$$

TABLE II
CHANNEL PARAMETERS

Shadowing	m_O	b_O	Ω_O
Frequent heavy shadowing (FHS)	1	0.063	0.0007
Average shadowing (AS)	5	0.251	0.279
Infrequent light shadowing (ILS)	10	0.158	1.29

Besides, $H_1 = \min\left(\frac{1/k_1^2-\gamma_0}{\gamma_0+1}, 1/k_1^2\right)$*,* $H_2 = \min\left(\frac{1/k_{R_p}^2-\gamma_0}{\gamma_0+1}, 1/k_{R_p}^2\right)$*, and* $H_3 = \min\left(\frac{1/k_{2i}^2-\gamma_0}{\gamma_0+1}, 1/k_{2i}^2\right)$*.* n_1*,* n_2*,* n_3 *and* n_4 *are the number of the terms,* $z_i = \frac{H_1}{2}\left(x_i+1\right)$ *represents the* i*-th zero of Legendre polynomials,* $z_\iota = \frac{H_2}{2}\left(x_\iota+1\right)$ *represents the* ι*-th zero of Legendre polynomials,* $z_\sigma = \frac{H_3}{2}\left(w_\sigma+1\right)$ *represents the* σ*-th zero of Legendre polynomials,* $z_\phi = \frac{H_2}{2}\left(w_\phi+1\right)$ *is the* ϕ*-th zero of Legendre polynomials,* w_i*,* w_ι*,* w_σ *and* w_ϕ *denote the Gaussian weight, respectively, which is seen in Table (25.4) of [47].*

Proof: Please see Appendix A. ■

C. Asymptotic Secrecy Outage Probability

To get the more insights of major parameters on the SOP in high SNR regime, the asymptotic investigations for the SOP will be derived in this subsection. When analyzing the asymptotic performance, which means $\bar{\gamma}_{LL} \to \infty$, $LL \in \left\{S_{1R_p}, S_{2iR_p}, R_pS_{2i}, R_pS_1\right\}$, in other words, $\frac{1}{\bar{\gamma}_{LL}} \to 0$, then using $\exp\left(-x\right) \underset{x\to 0}{\approx} 1-x$ and $\left(Ax+B\right) \underset{x\to 0}{\approx} B$, (29), (31), (33) and (35) can be re-written as (37), (38), (39) and (40), which are shown as at 7-th page and 8-th page, respectively.

From the asymptotic SOP analysis, the secrecy diversity order can be derived as

$$G_D = M. \tag{41}$$

From (37), (38), (39) and (40), we know that when $x_0 \le \min\left(H_1, H_2, H_3\right)$, the secrecy coding gain is given as (42), which can be found at the top of 8-th page.

IV. Numerical Results

Here, theoretical results are verified by the MC simulation results. Without of generality, we assume that $n_1 = n_2 = n_3 = n_4 = 16$, $\bar{\lambda}_{S_1R_p} = \bar{\lambda}_{S_{2i}R_p} = \bar{\lambda}_{R_pS_1} = \bar{\lambda}_{R_pS_{2i}} = \bar{\gamma}$, $\bar{\lambda}_{S_1E} = \bar{\lambda}_{S_{2i}E} = \bar{\lambda}_{R_pE} = \bar{\gamma}_E$, $\delta_{R_p}^2 = \delta_{E_j}^2 = \delta_{S_{2i}}^2 = \delta_{S_1}^2 = 1$, and $k_1 = k_{2i} = k_{R_p} = k$. Besides, the key parameters for the channel and system are presented in Table II [40] and Table III [42], respectively.

Fig. 2 illustrates the SOP versus $\bar{\gamma}$ for several shadow fading and impairments' level. In Fig. 2, we assume $\bar{\gamma}_E$ =0 dB, γ_0=0 dB, $L=1$, $N=1$ and $M=10$. From Fig. 2, firstly, we could derive that the simulation results are same with the theoretical investigations, which verify the rightness of our theoretical results. In addition, at high SNRs, the asymptotic derivations are tight across the simulation results, which in addition to show the rightness of the analysis. Moreover, in this figure, it

$$\Pr\left(C_{S_{11}} \le C_0\right) = \begin{cases} 1 - \frac{NH_1}{2} \sum\limits_{k_1=0}^{m_{S_1R_p,k}-1} \sum\limits_{t=0}^{k_1} \frac{\alpha_{m_{S_1R_p,k}} \left(1-m_{m_{S_1R_p,k}}\right)_{k_1} \left(-\delta_{m_{S_1R_p,k}}\right)^{k_1}}{k_1! t! \bar{\lambda}_{m_{S_1R_p,k}}^{k_1+1} \Delta_{m_{S_1R_p,k}}^{k_1-t+1} \bar{\lambda}_{S_2R_p}} \\ \times \sum\limits_{q=0}^{N-1} \binom{N-1}{q} (-1)^q \sum\limits_{p=0}^{t} \binom{p}{t} \left(1+k_{2i}^2\right)^p p! \sum\limits_{\xi_1=0}^{m_{S_1E}-1} \cdots \sum\limits_{\xi_L=0}^{m_{S_1E}-1} \Xi\left(L\right) \sum\limits_{i=1}^{n_1} w_i H_1\left(z_i\right), x_0 \le H_1 \\ 1, x_0 > H_1. \end{cases} \tag{29}$$

$$\Pr\left(C_{S_{22}} \le C_0\right) = \begin{cases} \frac{H_2}{2} \sum\limits_{q=0}^{N} \binom{N}{q} (-1)^q \sum\limits_{i=1}^{\rho\left(A_{R_pE}\right)} \sum\limits_{j=1}^{\tau_i\left(A_{R_pE}\right)} \frac{\chi_{i,j}\left(A_{R_pE}\right) \mu_{\langle i \rangle}^{-j}}{(j-1)!} \sum\limits_{\iota=1}^{n_2} w_\iota H_2\left(z_\iota\right), x_0 \le H_2 \\ 1, x_0 > H_2. \end{cases} \tag{31}$$

$$\Pr\left(C_{S_{12}} \le C_0\right) = \begin{cases} 1 - \frac{H_3}{2} \sum\limits_{q=1}^{N} \binom{N}{q} (-1)^{q-1} \sum\limits_{k_1=0}^{m_{S_2R_p}-1} \frac{\alpha_{S_2R_p} \left(1-m_{S_2R_p}\right)_{k_1} \left(-\delta_{S_2R_p}\right)^{k_1}}{(k_1!)^2 \bar{\lambda}_{S_2R_p}^{k_1+1}} \\ \times (k_1!) \sum\limits_{i=1}^{\rho\left(A_{S_{2i}E}\right)} \sum\limits_{j=1}^{\tau_i\left(A_{S_{2i}E}\right)} \frac{\chi_{i,j}\left(A_{S_{2i}E}\right) \mu_{\langle i \rangle}^{-j}}{(j-1)!} \sum\limits_{\sigma=1}^{n_3} w_\sigma H_3\left(z_\sigma\right), x_0 \le H_3 \\ 1, x_0 > H_3. \end{cases} \tag{33}$$

$$\Pr\left(C_{S_{21}} \le C_0\right) = \begin{cases} 1 - \frac{H_2}{2} \sum\limits_{k_1=0}^{m_{R_pS_1,k}-1} \sum\limits_{t=0}^{k_1} \frac{\alpha_{R_pS_1,k} \left(1-m_{R_pS_1,k}\right)_{k_1} \left(-\delta_{R_pS_1,k}\right)^{k_1}}{k_1! t! \bar{\lambda}_{R_pS_1,k}^{k_1+1} \Delta_{R_pS_1,k}^{k_1-t+1}} \\ \times \sum\limits_{i=1}^{\rho\left(A_{R_pE}\right)} \sum\limits_{j=1}^{\tau_i\left(A_{R_pE}\right)} \frac{\chi_{i,j}\left(A_{R_pE}\right) \mu_{\langle i \rangle}^{-j}}{(j-1)!} \sum\limits_{\varphi=1}^{n_4} w_\phi H_4\left(z_\phi\right), x_0 \le H_2 \\ 1, x_0 > H_2. \end{cases} \tag{35}$$

$$\overset{\infty}{\Pr}\left(C_{S_{11}} \le C_0\right) = \begin{cases} 1 - \frac{NH_1}{2} \sum\limits_{k_1=0}^{m_{S_1R_p,k}-1} \sum\limits_{t=0}^{k_1} \frac{\alpha_{m_{S_1R_p,k}} \left(1-m_{m_{S_1R_p,k}}\right)_{k_1} \left(-\delta_{m_{S_1R_p,k}}\right)^{k_1}}{k_1! t! \bar{\lambda}_{m_{S_1R_p,k}}^{k_1+1} \Delta_{m_{S_1R_p,k}}^{k_1-t+1} \bar{\lambda}_{S_2R_p}} \\ \times \sum\limits_{q=0}^{N-1} \sum\limits_{p=0}^{t} \sum\limits_{\xi_1=0}^{m_{S_1E}-1} \cdots \sum\limits_{\xi_L=0}^{m_{S_1E}-1} \sum\limits_{i=1}^{n_1} \Xi\left(L\right) w_i \binom{N-1}{q} (-1)^q \binom{p}{t} \left(1+k_{2i}^2\right)^p p! \\ \times \left[1 - \frac{\Delta_{m_{S_1R_p,k}} z^{t+\Lambda_{S_1E}}}{\left(1-k_1^2 z\right)\left(1-k_1^2 z\right)^{t+3-\Lambda_{S_1E}}}\right], x_0 \le H_1 \\ 1, x_0 > H_1. \end{cases} \tag{37}$$

$$\begin{aligned} &\overset{\infty}{\Pr}\left(C_{S_{22}} \le C_0\right) \\ &= \begin{cases} \frac{H_2}{2} \sum\limits_{q=0}^{N} \sum\limits_{i=1}^{\rho(A_Q)} \sum\limits_{j=1}^{\tau_i(A_Q)} \sum\limits_{\iota=1}^{n_2} \frac{w_\iota \chi_{i,j}(A_Q) \binom{N}{q} (-1)^q}{(j-1)! \mu_{\langle i \rangle}^{j}} \left(1 - \frac{q[z_\iota(1+\gamma_0)+\gamma_0]}{\bar{\lambda}_{R_pS_2}\left\{1-\left[k_{R_p}^2 z_\iota(1+\gamma_0)+\gamma_0\right]\right\}}\right) \left(\frac{z_\iota}{1-k_{R_p}^2 z_\iota}\right)^{j-1}, x_0 \le H_2 \\ 1, x_0 > H_2. \end{cases} \end{aligned} \tag{38}$$

$$\overset{\infty}{\Pr}\left(C_{S_{12}} \le C_0\right) = \begin{cases} 1 - \frac{H_3}{2} \sum\limits_{q=1}^{N} \sum\limits_{k_1=0}^{m_{S_2R_p}-1} \frac{\binom{N}{q} \alpha_{S_2R_p} \left(1-m_{S_2R_p}\right)_{k_1} \left(-\delta_{S_2R_p}\right)^{k_1}}{(-1)^{1-q} k_1! \bar{\lambda}_{S_2R_p}^{k_1+1}} \\ \times \sum\limits_{i=1}^{\rho\left(A_{S_{2i}E}\right)} \sum\limits_{j=1}^{\tau_i\left(A_{S_{2i}E}\right)} \sum\limits_{\sigma=1}^{n_3} \frac{\chi_{i,j}\left(A_{S_{2i}E}\right) w_\sigma}{(j-1)! \mu_{\langle i \rangle}^{j}} \left(1 - \frac{q[z_\sigma(1+\gamma_0)+\gamma_0]}{\left(1-k_{2i}^2[z_\sigma(1+\gamma_0)+\gamma_0]\right)\bar{\lambda}_{S_2R_p}}\right), x_0 \le H_3 \\ 1, x_0 > H_3. \end{cases} \tag{39}$$

This article has been accepted for publication in IEEE Transactions on Intelligent Vehicles. This is the author's version which has not been fully edited and content may change prior to final publication. Citation information: DOI 10.1109/TIV.2022.3215011

$$\overset{\infty}{\Pr}\left(C_{S_{21}} \le C_0\right) = \begin{cases} 1 - \frac{H_2}{2} \sum\limits_{k_1=0}^{m_O-1} \sum\limits_{t=0}^{k_1} \frac{\alpha_{R_pS_1,k}\left(1-m_{R_pS_1,k}\right)_{k_1}\left(-\delta_{R_pS_1,k}\right)^{k_1}}{k_1!t!\bar{\lambda}_{R_pS_1,k}^{k_1+1}\Delta_{R_pS_1,k}^{k_1-t+1}} \\ \times \sum\limits_{i=1}^{\rho\left(A_{R_pE}\right)} \sum\limits_{j=1}^{\tau_i\left(A_{R_pE}\right)} \sum\limits_{\varphi=1}^{n_4} \frac{w_\phi \chi_{i,j}\left(A_{R_pE}\right)}{(j-1)!\mu_{\langle i\rangle}^j} \left\{ \frac{z_\phi(1+\gamma_0)+\gamma_0}{1-k_{R_p}^2[z_\phi(1+\gamma_0)+\gamma_0]} \right\}^t \frac{e^{-\frac{z_\phi}{\left(1-k_{R_p}^2 z_\phi\right)\mu\langle i\rangle}} z_\phi^{j-1}}{\left(1-k_{R_p}^2 z_\phi\right)^{j+1}} \\ \times \left(1 - \frac{\Delta_{R_pS_1,k}[z_\phi(1+\gamma_0)+\gamma_0]}{1-k_{R_p}^2[z_\phi(1+\gamma_0)+\gamma_0]}\right), x_0 \le H_2 \\ 1, x_0 > H_2. \end{cases} \tag{40}$$

$$\begin{aligned} G_A = & \frac{NH_1}{2} \sum_{k_1=0}^{m_{S_1R_p,k}-1} \sum_{t=0}^{k_1} \frac{\alpha_{m_{S_1R_p,k}}\left(1-m_{m_{S_1R_p,k}}\right)_{k_1}\left(-\delta_{m_{S_1R_p,k}}\right)^{k_1}}{k_1!t!\left(\beta_{S_1R_p,k}-\delta_{S_1R_p,k}\right)^{k_1-t+1}} \\ & \times \sum_{q=0}^{N-1} \sum_{p=0}^{t} \sum_{\xi_1=0}^{m_{S_1E}-1} \cdots \sum_{\xi_L=0}^{m_{S_1E}-1} \sum_{i=1}^{n_1} \Xi\left(L\right) w_i \binom{N-1}{q} (-1)^q \binom{p}{t} \left(1+k_{2i}^2\right)^p p! \\ & + \frac{H_2}{2} \sum_{q=0}^{N} \sum_{i=1}^{\rho\left(A_{R_pE}\right)} \sum_{j=1}^{\tau_i\left(A_{R_pE}\right)} \sum_{\iota=1}^{n_2} \frac{w_\iota \chi_{i,j}\left(A_{R_pE}\right)\binom{N}{q}(-1)^q}{(j-1)!\mu_{\langle i\rangle}^j} \left(\frac{z_\iota}{1-k_{R_p}^2 z_\iota}\right)^{j-1} \\ & + \frac{H_3}{2} \sum_{q=1}^{N} \sum_{k_1=0}^{m_{S_2R_p}-1} \sum_{i=1}^{\rho\left(A_{S_{2i}E}\right)} \sum_{j=1}^{\tau_i\left(A_{S_{2i}E}\right)} \sum_{\sigma=1}^{n_3} \frac{\chi_{i,j}\left(A_{S_{2i}E}\right) w_\sigma \binom{N}{q} \alpha_{S_2R_p}\left(1-m_{S_2R_p}\right)_{k_1}\left(-\delta_{S_2R_p}\right)^{k_1}}{(j-1)!\mu_{\langle i\rangle}^j(-1)^{1-q}k_1!} \\ & + \frac{H_2}{2} \sum_{k_1=0}^{m_{R_pS_1,k}-1} \sum_{t=0}^{k_1} \sum_{i=1}^{\rho\left(A_{R_pE}\right)} \sum_{j=1}^{\tau_i\left(A_{R_pE}\right)} \sum_{\varphi=1}^{n_4} \frac{\alpha_{R_pS_1,k}\left(1-m_{R_pS_1,k}\right)_{k_1}\left(-\delta_{R_pS_1,k}\right)^{k_1} w_\phi \chi_{i,j}\left(A_{R_pE}\right) e^{-\frac{z_\phi}{\left(1-k_{R_p}^2 z_\phi\right)\mu\langle i\rangle}} z_\phi^{j-1}}{k_1!\left(\beta_{S_1R_p,k}-\delta_{S_1R_p,k}\right)^{k_1-t+1}(j-1)!\mu_{\langle i\rangle}^j\left(1-k_{R_p}^2 z_\phi\right)^{j+1}}. \end{aligned} \tag{42}$$

TABLE III
SYSTEM PARAMETERS

Parameters	Value
Satellite Orbit	GEO
Frequency band	$f = 2$ GHz
3dB angle	$\bar{\theta}_k = 0.8°$
Maximal Beam Gain	$G_{max} = 48$ dB
The Antenna Gain	$G_R = 4$ dB

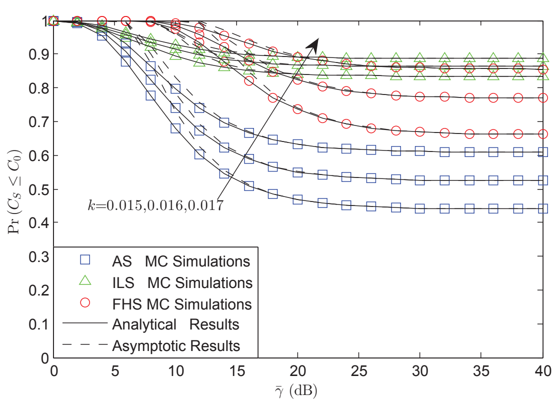

Fig. 2. SOP versus $\bar{\gamma}$ for different shadow fading and impairments' level with $\bar{\gamma}_E$ =0 dB, γ_0=0 dB, $L = 1$, $N = 1$ and $M = 10$.

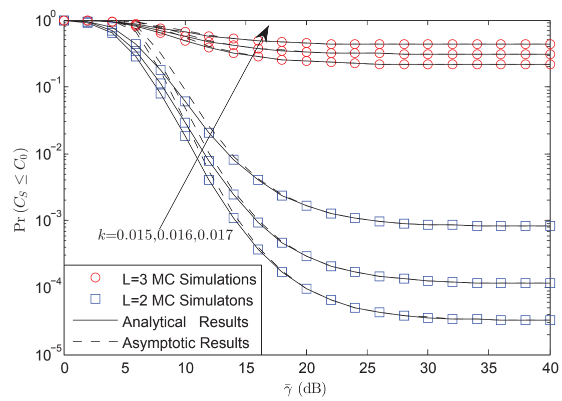

Fig. 3. SOP versus $\bar{\gamma}$ for different L and impairments' level with $\bar{\gamma}_E$ =-5 dB, γ_0=0 dB, $N = 1$ and $M = 10$ under AS scenario.

is very interesting that, the SOP for AS scenario is lower than that of FHS scenario as a result that when the channel suffers light fading, the SOP will be lower. However, we find that the SOP for ILS scenario is the worst, which results in that when the channel is under ILS shadowing, the channel quality for vehicle eavesdropper is the best. In ILS scenario, the impact of channel quality on vehicle eavesdroppers in superior to that of legitimate vehicle user, thus the SOP is the highest. Finally, the lower HIs' level will lead to a lower SOP.

Fig. 3 illustrates the SOP versus $\bar{\gamma}$ for several L and

This article has been accepted for publication in IEEE Transactions on Intelligent Vehicles. This is the author's version which has not been fully edited and content may change prior to final publication. Citation information: DOI 10.1109/TIV.2022.3215011

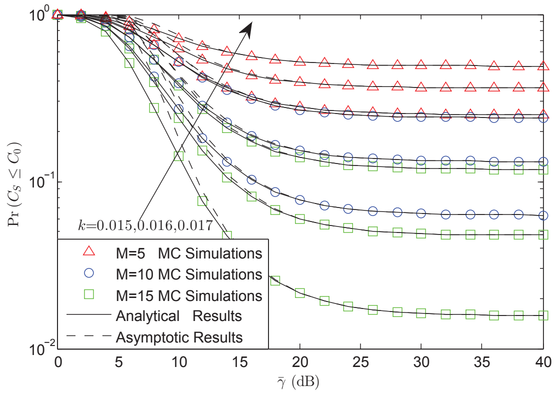

Fig. 4. SOP versus $\bar{\gamma}$ for different M and impairments' level with $\bar{\gamma}_E$ =-2 dB, γ_0=0 dB, $N = 1$ and $L = 1$ under AS scenario.

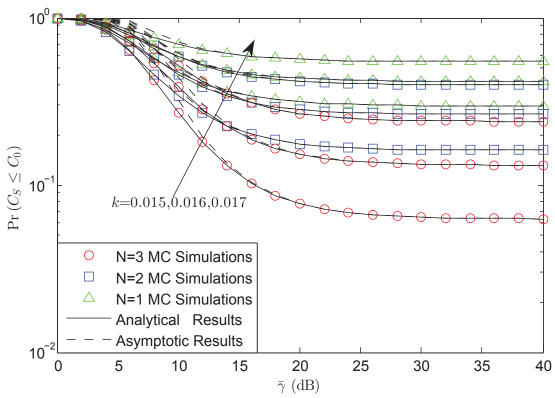

Fig. 5. SOP versus $\bar{\gamma}$ for different N and impairments' level with $\bar{\gamma}_E$ =-2 dB, γ_0=0 dB, $M = 10$ and $L = 1$ under AS scenario.

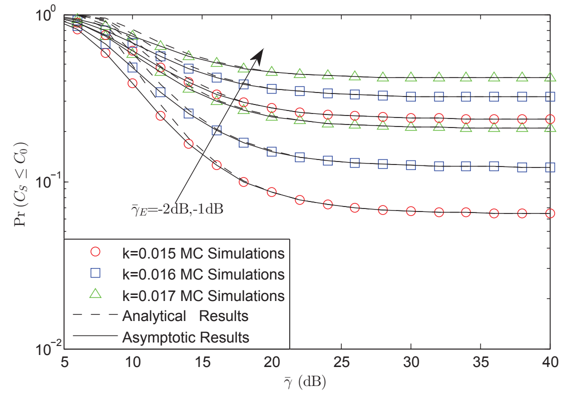

Fig. 6. SOP versus $\bar{\gamma}$ for different $\bar{\gamma}_E$ and impairments' level with $N = 1$, γ_0=0 dB, $M = 10$ and $L = 1$ under AS scenario.

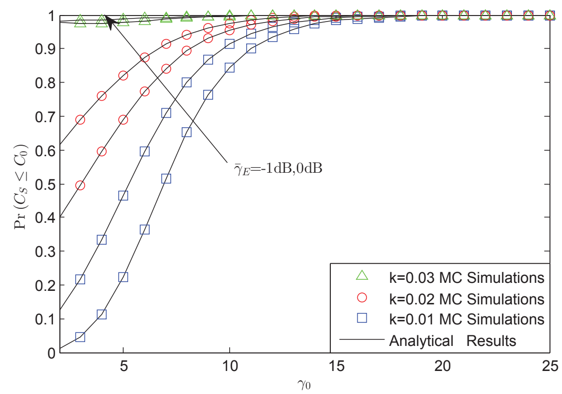

Fig. 7. SOP versus γ_0 for different $\bar{\gamma}_E$ and impairments' level with $N = 3$, $M = 10$ and $L = 1$ under AS scenario.

impairments' level. In Fig. 3, we has the assumption that $\bar{\gamma}_E$ =-5 dB, γ_0=0 dB, $N = 1$ and $M = 10$ under AS scenario. The same results with Fig. 2, the simulations results are also same with theoretical analysis through the whole SNRs, moreover, the asymptotic analysis are still tight across the theoretical results in high SNR regime. From this figure, it is observed that the SOP with larger L is lower than that of the smaller L. There is a larger gap between the considered two cases, which implies that the number of vehicle eavesdroppers has a great impact on the SOP performance.

Fig. 4 depicts the SOP versus $\bar{\gamma}$ for several M and impairments' level. In Fig. 4, we have $\bar{\gamma}_E$ =-2 dB, γ_0=0 dB, $N = 1$ and $L = 1$ under AS scenario. From Fig. 4, it can be gotten that, the SOP will be lower when the number of terrestrial relay increases. However, when compared with Fig. 3, we can observe that the impact of the vehicle eavesdroppers' number is superior to that of relays' number. At last, the SOP will have a lower value when suffering the the light impairments.

Fig. 5 shows the SOP versus $\bar{\gamma}$ for different N and impairments' level. In Fig. 5, we let $\bar{\gamma}_E$ =-2 dB, γ_0=0 dB, $M = 10$ and $L = 1$ under AS scenario. From this figure, it is can be gotten that with a larger terrestrial vehicle users' number, the SOP will be lower as a result of that multiple legitimate vehicle users joint in to transmit the signals. At this scenario, the legitimate vehicle users are the major power. So this simulation figure appears.

Fig. 6 plots the SOP versus $\bar{\gamma}$ for several $\bar{\gamma}_E$ and impairments' level with $N = 1$, γ_0=0 dB, $M = 10$ and $L = 1$ under AS scenario. From this figure, we can find that the SOP with lower $\bar{\gamma}_E$ will lead to a lower SOP owing to that the quality of the eavesdroppers gets worse. The reason is that the larger vehicle eavesdropping power will lead to a larger SOP.

Fig. 7 illustrates the SOP versus γ_0 for several $\bar{\gamma}_E$ and impairments' level with $N = 3$, $M = 10$ and $L = 1$ under AS scenario. It can be derived that, the SOP will grow to 1 after a special value under the HIs scenario, in addition, it also could be found that this particular value only has relationship with HIs' level, which has the meaning that a lower HIs level brings a larger value. In addition, we find that the $\bar{\gamma}_E$ value does not influence the special value.

V. Conclusions

This work studied the secrecy performance for the ISMT-TRNs along with opportunistic relay selection scheme, which consisted of many legitimate vehicle users and several vehicle eves. More importantly, the closed-form and asymptotic expressions for the SOP were obtained based on the multiple vehicle eavesdroppers and two-way technology. In addition, the channel parameters and system parameters have been observed for the considered SOP. The results have shown that the channel fading, the number of the vehicle eavesdroppers, the number of the two-way relays, the number of the legitimate vehicle users and the eavesdroppers' power have a great impact on the SOP. Especially, the variation for the HIs' level has serious effects on the secure system performance.

APPENDIX A
PROOF OF THEOREM 1

For $S_1 \to S_2$ secrecy transmission link:

$$\begin{aligned}\Pr\left(C_{S_1} \le C_0\right) = &\Pr\left(C_{S_{11}} \le C_0\right) + \Pr\left(C_{S_{22}} \le C_0\right)\\ &- \Pr\left(C_{S_{11}} \le C_0\right)\Pr\left(C_{S_{22}} \le C_0\right). \end{aligned}\quad (43)$$

For $S_2 \to S_1$ secrecy transmission link:

$$\begin{aligned}\Pr\left(C_{S_2} \le C_0\right) = &\Pr\left(C_{S_{12}} \le C_0\right) + \Pr\left(C_{S_{21}} \le C_0\right)\\ &- \Pr\left(C_{S_{12}} \le C_0\right)\Pr\left(C_{S_{21}} \le C_0\right). \end{aligned}\quad (44)$$

At first, by utilizing the help of $C_{S_{11}} = \left[\log_2\left(1+\gamma_{S_1\to R_p}\right) - \log_2\left(1+\gamma_{S_1\to E}\right)\right]^+$, $\Pr\left(C_{S_{11}} \le C_0\right)$ can be obtained as

$$\begin{aligned}&\Pr\left(C_{S_{11}} \le C_0\right)\\ &= \Pr\left[\log_2\left(1+\gamma_{S_1\to R_p}\right) - \log_2\left(1+\gamma_{S_1\to E}\right) < \log_2\left(1+\gamma_0\right)\right]\\ &= \Pr\left[\gamma_{S_1\to R_p} < \gamma_0 + \left(\gamma_0+1\right)\gamma_{S_1\to E}\right]. \end{aligned}\quad (45)$$

From (45), we know the most important thing is to get the CDF for $\gamma_{S_1\to R_p}$ and the PDF for $\gamma_{S_1\to E}$. With the help of (9) and [42], the PDF for $\gamma_{S_1\to E}$ can be obtained as

$$\begin{aligned}f_{\gamma_{S_1\to E}}(x) &= \frac{1}{\left(1-k_1^2 x\right)^2} f_{\lambda_{S_1E}}\left(\frac{x}{1-k_1^2 x}\right)\\ &= \frac{\sum\limits_{\xi_1=0}^{m_{S_1E}-1}\cdots\sum\limits_{\xi_L=0}^{m_{S_1E}-1}\frac{\Xi(L)}{\exp\left(\frac{\Delta_{S_1E}x}{1-k_1^2x}\right)}\left(\frac{x}{1-k_1^2x}\right)^{\Lambda_{S_1E}-1}}{\left(1-k_1^2x\right)^2}. \end{aligned}\quad (46)$$

By the similar method and (7), the CDF for $\gamma_{S_1\to R_p}$ can be obtained as

$$\begin{aligned}F_{\gamma_{S_1\to R_p}}(x) &= \Pr\left(\frac{\lambda_{S_1R_p}}{\lambda_{S_1R_p}k_1^2 + \lambda_{S_2R_p}\left(1+k_{2i}^2\right)+1} \le x\right)\\ &= \Pr\left(\lambda_{S_1R_p} \le \lambda_{S_2R_p}C + D\right), \end{aligned}\quad (47)$$

where $C = \frac{\left(1+k_{2i}^2\right)x}{1-k_1^2x}$ and $D = \frac{x}{1-k_1^2x}$.

Then by submitting (25) with $O = S_1R_p$ and (18) with $X = S_2R_p$ into (47), the CDF for $F_{\gamma_{S_1\to R_p}}(x)$ is given by

$$\begin{aligned}&F_{\gamma_{S_1\to R_p}}(x)\\ &= 1 - \sum_{k_1=0}^{m_{S_1R_p,k}-1}\sum_{t=0}^{k_1}\frac{\alpha_{m_{S_1R_p,k}}\left(1-m_{m_{S_1R_p,k}}\right)_{k_1}\left(-\delta_{m_{S_1R_p,k}}\right)^{k_1}}{k_1!\bar{\lambda}_{m_{S_1R_p,k}}^{k_1+1}\Delta_{m_{S_1R_p,k}}^{k_1-t+1}}\\ &\times\frac{N}{\bar{\lambda}_{S_2R_p}}\sum_{q=1}^{N-1}\binom{N-1}{q}(-1)^q\exp\left(-\Delta_{m_{S_1R_p,k}}D\right)\sum_{p=0}^{t}\binom{p}{t}\\ &\times C^pD^{t-p}p!\left(\Delta_{m_{S_1R_p,k}}C + \frac{q+1}{\bar{\lambda}_{S_2R_p}}\right)^{-p-1}. \end{aligned}\quad (48)$$

Recalling (45), (45) can be re-written as

$$\begin{aligned}&\Pr\left(C_{S_{11}} \le C_0\right)\\ &= \int_0^\infty F_{\gamma_{S_1\to R_p}}\left[\gamma_0 + \left(\gamma_0+1\right)y\right] f_{\gamma_{S_1\to E}}(y)\,dy. \end{aligned}\quad (49)$$

It should be noted that in (48) and (46), y should be satisfied with the following condition, which means $y \le 1/k_1^2$ and $y < \frac{1/k_1^2-\gamma_0}{\gamma_0+1}$, which results in that (49) changes to

$$\begin{aligned}&\Pr\left(C_{S_{11}} \le C_0\right)\\ &= \int_0^{H_1} F_{\gamma_{S_1\to R_p}}\left[\gamma_0 + \left(\gamma_0+1\right)y\right] f_{\gamma_{S_1\to E}}(y)\,dy\\ &+ \int_{H_1}^{H^1} f_{\gamma_{S_1\to E}}(y)dy, \end{aligned}\quad (50)$$

where $H^1 = \max\left(\frac{1/k_1^2-\gamma_0}{\gamma_0+1}, 1/k_1^2\right)$.

However, try the authors' best efforts, it is too hard to derive the closed-form expression of (50). Based on [1] and utilizing the Gaussian-Chebyshev quadrature [47, eq. 25.4.38], (50) could re-given by

$$\begin{aligned}&\Pr\left(C_{S_{11}} \le C_0\right)\\ &= 1 - \int_0^{H_1}\left\{1 - F_{\gamma_{S_1\to R_p}}\left[\gamma_0 + \left(\gamma_0+1\right)y\right]\right\} f_{\gamma_{S_1\to E}}(y)\,dy. \end{aligned}\quad (51)$$

In addition, it is mentioned that, when $x_0 > H_1$, $\Pr\left(C_{S_{11}} \le C_0\right)$ is always 1 for the reason of the HIs' impact.

Then, by submitting (48) and (46) into (51), after some mathematical steps, (29) will be derived.

Then, with the similar method, the closed-form expressions for $\Pr\left(C_{S_{22}} \le C_0\right)$, $\Pr\left(C_{S_{12}} \le C_0\right)$ and $\Pr\left(C_{S_{21}} \le C_0\right)$ can be obtained as (31), (33) and (35). Finally, by submitting (29), (31), (33) and (35) into (28), the closed-form expression for $\Pr\left(C_S \le C_0\right)$ will be derived.

Thus, the proof is completed.

REFERENCES

[1] K. Guo, *et al.*, "NOMA-based cognitive satellite terrestrial relay network: Secrecy performance under channel estimation errors and hardware impairments," *IEEE Internet of Things J.*, early access, pp. 1-1, Mar. 2022.

[2] K. Y. Jo, *Satellite Communications Netwowrk Design and Analysis*. Norwood, MA, USA: Artech House, 2011.

[3] O. Kodheli, E. Lagunas, N. Maturo, S. K. Sharma, B. Shankar, J. F. M. Montoya, J. C. M. Duncan, D. Spano, S. Chatzinotas, S. Kisseleff, J. Querol, L. Lei, T. X. Vu, and G. Goussetis, "Satellite communications in the new space era: A survey and future challenges," *IEEE Commun. Surveys Tut.*, vol. 23, no. 1, pp. 70-109, Firstquarter, 2021.

[4] K. Guo, M. Lin, B. Zhang, J.-B. Wang, Y. Wu, W.-P. Zhu, and J. Cheng, "Performance analysis of hybrid satellite-terrestrial cooperative networks with relay selection," *IEEE Trans. Vehi. Technol.*, vol. 69, no. 8, pp. 9053-9067, Aug. 2020.

[5] ETSI TS 102 585 V1.1.2, "Digital Video Broadcasting (DVB); System specifications for Satellite services to Handheld devices (SH) below 3 GHz," Apr. 2008.

[6] M. Lin, Q. Huang, T. de. Cola, J.-B. Wang, J. Wang, M. Guizani, and J.-Y. Wang, "Integrated 5G-satellite networks: A perspective on physical layer relibility and security," *IEEE Wireless Commun.*, vol. 27, no. 6, pp. 152-159, Dec. 2020.

[7] K. An, T. Liang, G. Zheng, X. Yan, Y. Li, S. Chatzinotas, "Performance Limits of Cognitive-Uplink FSS and Terrestrial FS for Ka-Band", *IEEE Trans. Aerospace and Electronic Systems*, vol. 55, no. 5, pp. 2604-2611, Oct. 2019.

[8] K. Guo, K. An, F. Zhou, T.-A Tsiftsis, G. Zheng, and S. Chatzinotas, "On the secrecy performance of NOMA-based integrated satellite multiple-terrestrial relay networks with hardware impairments," *IEEE Trans. Vehi. Technol.*, vol. 70, no. 4, pp. 3661-3676, Apr. 2021.

[9] K. An, M. Lin, J. Ouyang, Y. Huang, and G. Zheng, "Symbol error analysis of hybrid satellite-terresrial cooperative networks with cochannel interference," *IEEE Commun. Lett.*, vol. 18, no. 11, pp. 1947-1950, Nov. 2014.

[10] K. Guo, K. An, B. Zhang, Y. Huang, and G. Zheng, "Outage analysis of cognitive hybrid satellite-terrestrial networks with hardware impairments and multi-primary users," *IEEE Wireless Commun. Lett.*, vol. 7, no. 5, pp. 816-819. Oct. 2018.

[11] K. An, M. Lin, T. Liang, J.-B. Wang, J. Wang, Y. Huang, and A. L. Swindlehurst, "Performance analysis of multi-antenna hybrid satellite-terrestrial relay networks in the presence of interference," *IEEE Trans. Commun.*, vol. 63, no. 11, pp. 4390-4404, Nov. 2015.

[12] Y. Zhang, X. Li, H. Zhang, *et al.*, "Overlay cognitive ABCom-NOMA based ITS: An in-depth secrecy analysis," *IEEE Trans. Intelligent Transportation Syst.*, early access, pp. 1-12, Jan. 2022.

[13] K. Guo and K. An, "On the performance of RIS-assisted integrated satellite-UAV-terrestrial networks with hardware impairments," *IEEE Wireless Commun. Lett.*, vol. 11, no. 1, pp. 131-135, Jan. 2022.

[14] P. K. Sharma, P. K. Upadhyay, D. B. costa, P. S. Bithas, and A. G. Kanatas, "Performance analysis of overlay spectrum sharing in hybrid satellite-terrestrial systems with secondary network selection," *IEEE Trans. Wireless Commun.*, vol. 16, no. 10, pp. 6586-6601, Oct. 2017.

[15] P. K. Upadhyay and P. K. Sharma, "Max-max user-relay selection scheme in multiuser and multirelay hybrid satellite-terrestrial relay systems," *IEEE Commun. Lett.*, vol. 20, no. 2, pp. 268-271, Jan. 2016.

[16] K. Guo, *et al.*, "Performance analysis of two-way multiantenna multirelay networks with hardware impairments," *IEEE Access*, vol. 5, pp. 15971-15980, Aug. 2017.

[17] K. Guo, *et al.*, "Performance analysis of two-way satellite multiterrestrial relay networks with hardware impairments," *Sensors*, vol. 18, no. 5, pp. 1-19, May 2018.

[18] K. Guo, *et al.*, "Secrecy performance of satellite wiretap channels with multi-user opportunistic scheduling," *IEEE Wireless Commun. Lett.*, vol. 7, no. 6, pp. 1054-1057, Dec. 2018.

[19] K. Guo, *et al.*, "On the performance of the uplink satellite multiterrestrial relay networks with hardware impairments and interference," *IEEE Syst. J.*, vol. 13, no. 3, pp. 2297-2308, Sep. 2019.

[20] X. Tang, *et al.*, "On the performance of two-way multiple relay nonorthogonal multiple access based networks with hardware impairments," *IEEE Access*, vol. 7, pp. 128896-128909, Sep. 2019.

[21] X. Wu, *et al.*, "Outage performance for multiuser threshold-based DF satellite relaying," *IEEE Access*, vol. 7, pp. 103142-103152, Jul. 2019.

[22] Y. Zhao, L. Xie, H. Chen, and K. Wang, "Ergodic channel capacity analysis of downlink in the hybrid satellite-terrestrial cooperative system," *Wireless Personal Commun.*, vol. 96, no. 3, pp. 3799-3815, Oct. 2017.

[23] K. Guo, *et al.*,"Performance analysis of two-way satellite terrestrial relay networks with hardware impairments," *IEEE Wireless Commun. Lett.*, vol. 6, no. 4, pp. 430-433, 2017.

[24] W. Zeng, *et al.*, "Two-way hybrid terrestrial-satellite relaying systems: Performance analysis and relay selection," *IEEE Trans. Vehi. Technol.*, vol. 68. no. 7, pp. 7011-7023, 2019.

[25] X. Tang, *et al.*, "On the performance of two-way multiple relay nonorthogonal multiple access based networks with hardware impairments," *IEEE Access*, vol. 7, pp. 128896-128909, 2019.

[26] B. Li, Z. Fei, C. Zhou, and Y. Zhang, "Physical layer security in space information networks: A survey," *IEEE Internet of Things Journal*, vol. 7, no. 1, pp. 33-52, Jan. 2020.

[27] Z. Lin, M. Lin, J.-B. Wang, T. de. Cola, and J. Wang, "Joint beamforming and power allocation for satellite-terrestrial integrated networks with non-orthogonal multile access," *IEEE J. Sel. Topic S. Proc.*, vol. 13, no. 3, pp. 657-670, Jun. 2019.

[28] B. Li, *et al.*, "Robust chance-constrained secure transmission for cognitive satellite-terrestrial networks", *IEEE Trans. Vehi. Technol.*, vol. 67, no. 5, pp. 4208-4219, 2018.

[29] Z. Lin, *et al.*, "Secrecy-energy efficient hybrid beamforming for satellite-terrestrial integrated networks," *IEEE Trans. Commun.*, vol. 69, no. 3, pp. 6345-6360, 2021.

[30] Z. Lin, *et al.*, "Robust secure beamforming for wireless powered cognitive satellite-terrestrial networks," *IEEE Trans. Cognitive Commun. Networking*, vol. 7, no. 2, pp. 567-580, 2021.

[31] K. An, M. Lin, J. Ouyang and W.-P. Zhu, "Secure transmission in cognitive satellite terrestrial networks," *IEEE J. Sel. Areas in Commun.*, vol. 34, no. 11, pp. 3025-3037. Nov. 2016.

[32] D. Yang, B. Ren, H. Li, X. Wang, and K. Guo, "Secrecy performance of two-way integrated satellite terrestrial relay networks with multiple users," *Electronics Lett.*, vol. 58, no. 16, pp. 636-638, Aug. 2022.

[33] X. Li, M. Huang, Y. Liu, V. G. Menon, A. Paul, and Z. Ding, "I/Q imbalance aware nonlinear wireless-powered relaying of B5G networks: Security and reliability analysis," *IEEE Trans. Network Science and Engineering*, vol. 8, no. 4, pp. 2995-3008, Oct.-Dec. 2021.

[34] X. Li, Y. Zheng, M. D. Alshehri, L. Hai, V. Balasubramanian, M. Zeng, and Gaofeng Nie, "Cognitive AmBC-NOMA IoV-MTS networks with IQI: Reliability and security analysis," *IEEE Trans. Intelligent Transportation Systems*, early access, pp. 1-12, Sep. 2021.

[35] X. Li, J. Li, Y. Liu, Z. Ding, and A. Nallanathan, "Residual transceiver hardware impairments on cooperative NOMA networks," *IEEE Trans. Wireless Commun.*, vol. 19, no. 1, pp. 680-695, Jan. 2020.

[36] E. Bjornson, M. Matthaiou, and M. Debbah, "A new look at dual-hop relaying: Performance limits with hardware impairments," *IEEE Trans. Commun.*, vol. 61, no. 11, pp. 4512-4525, Nov. 2013.

[37] J. Zhang, L. Dai, X. Zhang, E. Bjornson, and Z. Wang, "Achievable rate of Rician large-scale MIMO channels with transceiver hardware impairments," *IEEE Trans. Veh. Technol.*, vol. 65, no. 10, pp. 8800-8806, Dec. 2016.

[38] N. Maletic, M. Cabarkapa, N. Neskovic, and D. Budimir, "Hardware impairments impact on fixed-gain AF relaying performance in nakagami-m fading," *Electronics Letters*, vol. 52, no. 2, pp. 121-122, Jan. 2016.

[39] T. T. Duy, T. Q. Duong, D. B. Costa, *et al.*, "Proactive relay selection with joint impact of hardware impairments and co-channel interference," *IEEE Trans. Commun.*, vol. 63, no. 5, pp. 1594-1606, May 2015.

[40] K. Guo, *et al.*, "On the performance of LMS communication with hardware impairments and interference," *IEEE Trans. Commun.*, vol. 67, no. 2, pp. 1490-1505, Feb. 2019.

[41] X. Li, Y. Zheng, W. U. Khan, M. Zeng, D. Li, R. G. K. and L. Li, "Physical layer security of cognitive ambient backscatter communications for green internet-of-things," *IEEE Trans. Green Commun. Networking*, vol. 5, no. 3, pp. 1066-1076, Sep. 2021.

[42] K. Guo, K. An, B. Zhang, *et al.*, "Physical layer security for multiuser satellite communication systems with threshold-based scheduling scheme," *IEEE Trans. Vehi. Technol.*, vol. 69, no. 5, pp. 5129-5141, May 2020.

[43] B. Li, Z. Fei, X. Xu, and Z. Chu, "Resource allocations for secure cognitive satellite-terrestrial networks," *IEEE Wireless Commun. Lett.*, vol. 7, no. 1, pp. 78-81, Feb. 2018.

[44] H. Wu, *et al.*, "Secrecy performance of hybrid satellite-terrestrial relay systems with hardware impairments," *IEEE ICC 2019*, Shanghai China, May. 2019, pp. 1-6.

[45] J. Arnau, D. Christopoulos, S. Chatzinotas, C. Mosquera, and B. Ottersten, "Performance of the multibeam satellite return link with correlated rain attenuation," *IEEE Trans. Wireless Commun.*, vol. 13, no. 11, pp. 6286-6299, Nov. 2014.

[46] I. S. Gradshteyn, I. M. Ryzhik, A. Jeffrey, and D. Zwillinger, "Table of integrals, series and products," *7thed. Amsterdam*, Boston: Elsevier, 2007.

[47] M. Abramowitz and I. A. Stegun, *Handbook of Mathematical Functions With Formulas, Graphs, and Mathematical Tables*, 9th ed. New York, NY, USA: Dover, 1972.

Kefeng Guo (S'12-M'18) received his B.S. degree from Beijing Institute of Technology, Beijing, China, in 2012, the M.S. degree from PLA University of Science and Technology, Nanjing, China, in 2015 and the Ph.D. degree in Army Engineering University of PLA in 2018. He is a Lecturer in School of Space Information, Space Engineering University. He is also the associate professor in the College of Electronic and Information Engineering, Nanjing University of Aeronautics and Astronautics. He has authored or coauthored nearly 60 research papers in international journals and conferences. His research interests focus on cooperative relay networks, MIMO communications systems, multiuser communication systems, satellite communication, hardware impairments, cognitive radio, NOMA technology and physical layer security. He was the Guest Editor for the special issue onIntegration of SatelliteC AerialC Terrestrial Networks of Sensors.

Dr. Guo has been the TPC member of many IEEE sponsored conferences, such as IEEE ICC, IEEE GLOBECOM and IEEE WCNC.

Xingwang Li (S'12-M'15-SM'20) received the M. Sc. and Ph. D. degrees from University of Electronic Science and Technology of China and Beijing University of Posts and Telecommunications in 2010 and 2015. From 2010 to 2012, he worked at Comba Telecom Ltd. In Guangzhou China, as an engineer. He spent one year from 2017 to 2018 as a visiting scholar at Queen's University Belfast, Belfast, UK. He is currently an Associated Professor with the School of Physics and Electronic Information Engineering, Henan Polytechnic University, Jiaozuo China. His research interests span wireless communication, intelligent transport system, artificial intelligence, Internet of things.

Dr. Li has served as many TPC members, such as the IEEE Globecom, IEEE ICC, IEEE WCNC, IEEE VTC, IEEE ICCC etc. He has also served as the Co-Chair for the IEEE/IET CSNDSP 2020 of the Green Communications and Networks Track. He also serves as an Editor on the Editorial Board for IEEE Transactions on Intelligent Transportation Systems, IEEE Transactions on Vehicular Technology, IEEE Systems Journal, Physical Communication. He was the Guest Editor for the special issue on Computational Intelligence and Advanced Learning for Next-Generation Industrial IoT of IEEE Transactions on Network Science and Engineering, "Recent Advances in Physical Layer Technologies for 5G-Enabled Internet of Things" of the Wireless Communications and Mobile Computing. He has served as many TPC members, such as IEEE ICC, GLOBECOM, WCNC, VTC, ICCC, etc. He is also the Co-Chair of IEEE/IET CSNDSP 2020 of the Green Communications and Networks track.

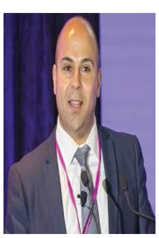

Mamoun Alazab is an Associate Professor at the College of Engineering, IT and Environment at Charles Darwin University, Australia. He is the recipient of the prestigious award: NT Young Tall Poppy (2021) of the year from the Australian Institute of Policy and Science (AIPS), and the Japan Society for the Promotion of Science (JSPS) fellowship through the Australian Academy of Science. He is a cyber security researcher and practitioner with industry and academic experience. He has more than 300 research papers (more than 90 % in Q1 and in the top 10 % of Journal articles, and more than 100 in IEEE/ACM Transactions) and 11 authored/edited books. He is a Senior Member of the IEEE, and the founding chair of the IEEE Northern Territory (NT) Subsection. He serves as the Associate Editor of IEEE Transactions on Computational Social Systems, IEEE Transactions on Network and Service Management (TNSM), IEEE Internet of Things Journal, ACM Digital Threats: Research and Practice, and Complex & Intelligent Systems.

Rutvij H. Jhaveri (Senior Member, IEEE) is an experienced educator and researcher working in the Department of Computer Science & Engineering, Pandit Deendayal Energy University, Gandhinagar, India. He conducted his Postdoctoral Research at Delta-NTU Corporate Lab for Cyber-Physical Systems, Nanyang Technological University, Singapore. He completed his PhD in Computer Engineerng in 2016. In 2017, he was awarded with prestigious Pedagogical Innovation Award by Gujarat Technological University. Currently, he is co-investigating a funded project from GUJCOST. He was ranked among top 2% s5ientists around the world in 2021. He has 2200+ Google Scholar citations with h-index 25. Apart from serving as an editor/ guest editor in various journals of repute, he also serves as a reviewer in several international journals and also as an advisory/TPC member in renowned international conferences. He authored 125+ articles including the IEEE/ACM Transactions and flagship IEEE/ACM conferences. Moreover, he has several national and international patents and, copyrights to his name. He also possesses memberships of various technical bodies such as ACM, CSI, ISTE, IDES and others. He is a member of the Advisory Board in Symbiosis Institute of Digital and Telecom Management, Manav Rachna Group and Sandip University since 2022. He is an editorial board member in several Hindawi and Springer journals. He also served as a committee member in "Smart Village Project" - Government of Gujarat, at the district level during the year 2017. His research interests are Cyber Security, IoT systems, SDN and Smart Healthcare.

Kang An received the B.S. degree from Nanjing University of Aeronautics and Astronautics, Nanjing, China, in 2011, the M.S. degrees from the PLA University of Science and Technology, Nanjing, China and the Ph.D. degree in Army Engineering University of PLA in 2017. He is currently an associate professor in The Sixty-third Research Institute, National University of Defense Technology, Nanjing. His research interests include cooperative communication, satellite communication, cognitive radio and physical layer security.